

**Transfer of Glucose Hydrogens via Acetyl-CoA, Malonyl-CoA and NADPH to Fatty Acids
during *de novo* Lipogenesis**

Getachew Debas Belew¹, Joao Silva¹, Joao Rito¹, Ludgero Tavares¹, Ivan Viegas^{1,2}, Jose Teixeira¹,
Paulo J. Oliveira¹ Maria Paula Macedo^{3,4,5} and John G. Jones^{1,4*}

¹CNC - Center for Neurosciences and Cell Biology, UC-Biotech, University of Coimbra, Portugal

²Centre for Functional Ecology, Department of Life Sciences, University of Coimbra, Portugal

³CEDOC-Chronic Diseases Research Center, NOVA Medical School / Faculdade de Ciências
Médicas, Universidade Nova de Lisboa, Lisboa, Portugal

⁴APDP-Portuguese Diabetes Association, Lisbon Portugal

⁵Department of Medical Sciences, Universidade Aveiro, Aveiro, Portugal

***Address for Correspondence:**

John G. Jones, Ph.D.

Center for Neurosciences and Cell Biology

UC-Biotech, Biocant Park Nucleo 8, Lote 4,

3060-197, Cantanhede, Portugal

email: john.griffith.jones@gmail.com

Word Count: 4090

Keywords: *de novo* lipogenesis, pentose phosphate pathway, ²H NMR.

Abstract (239 words):

Deuterated water ($^2\text{H}_2\text{O}$) is widely used for measuring *de novo* lipogenesis (DNL). ^2H is incorporated into fatty acids via exchange between body water and the hydrogens of acetyl-CoA, malonyl-CoA and NADPH. Previous studies concluded that these exchanges are incomplete therefore fatty acid ^2H -enrichment requires correcting. In mice, we measured the ^2H -enrichment of fatty acid positions 2, 3 and methyl hydrogens from $[\text{U-}^2\text{H}_7]\text{glucose}$ to determine ^2H -transfer from glucose to fatty acid via malonyl-CoA, NADPH and acetyl-CoA, respectively. Positional fatty acid ^2H -enrichments were compared to ^{13}C -enrichment of the same sites from an equivalent amount of $[\text{U-}^{13}\text{C}_6]\text{glucose}$ provided alongside the $[\text{U-}^2\text{H}_7]\text{glucose}$ tracer.

Transfer of glucose ^2H to fatty acid position 2 and methyl sites was low (^2H enrichment of 0.06 ± 0.01 and 0.14 ± 0.01 relative to ^{13}C) indicating extensive exchange at both malonyl- and acetyl-CoA, respectively. Transfer of glucose ^2H into fatty acid position 3 was more extensive (0.46 ± 0.04 relative to ^{13}C , $p < 10^{-5}$ versus position 2) indicating a more limited exchange of those glucose hydrogens that were transferred via NADPH. However, mice provided with $[\text{U-}^{13}\text{C}_6]\text{glucose}$ and $^2\text{H}_2\text{O}$ had equivalent ^2H -enrichments of fatty acid positions 2 and 3 suggesting that in this setting, NADPH and body water ^2H had exchanged extensively. This is explained by contributions of substrates other than exogenous glucose to DNL coupled with their extensive ^2H -enrichment from $^2\text{H}_2\text{O}$ prior to DNL. Under such conditions, ^2H -enrichment of fatty acids from $^2\text{H}_2\text{O}$ do not need correction.

Introduction:

There is currently high interest in the measurement of *de novo* lipogenesis (DNL) to better understand its role in the dyslipidemia of diseases such as Type 2 diabetes and fatty liver disease (1-3). Fractional DNL rates can be measured from incorporation of deuterated water ($^2\text{H}_2\text{O}$) into fatty acids (4, 5) – an inexpensive and simple method that can be applied to humans, animal models and cell cultures. ^2H enrichment of fatty acids from $^2\text{H}_2\text{O}$ is conventionally measured by mass-spectrometry (MS), where all the fatty acid chain hydrogens are considered as a single traceable entity (4). While this provides amplification of the m+1 signal arising from ^2H incorporation, it does not resolve the carbon-bound fatty acid hydrogens according to their metabolic sources (see Figure 1). It was reported that in rats, about 30% of plasma triglyceride palmitate hydrogens had not exchanged with ^2H -body water (6, 7) while for palmitate derived from cultured cells, this non-exchanged fraction was even higher (8). Therefore for DNL measurement, the ^2H -enrichment of fatty acids measured by MS needs to be corrected by a pre-determined factor related to the number of deuterium atoms that were incorporated per molecule of fatty acid, referred to as N (6). Stoichiometric ^2H -enrichment of fatty acids from $^2\text{H}_2\text{O}$ is conditional on full exchange between the hydrogens of water and those of the acetyl-CoA methyls, the malonyl-CoA methylenes, and the reducing hydrogen of NADPH. A less than theoretical ^2H -enrichment of the fatty acids implies that hydrogen exchange is incomplete, but to what degree this occurs for each of the metabolic precursors is not known. To address this, we provided mice with [U- $^2\text{H}_7$]glucose and performed ^2H NMR analysis of liver triglyceride (5, 9, 10) to determine the extent to which the ^2H were transferred into positions 2, 3 and the terminal methyl hydrogens of hepatic fatty acids: each position reflecting ^2H transfer from glucose via malonyl-CoA, NADPH and acetyl-CoA, respectively. Our data indicate that there was a substantial transfer of glucose hydrogen to newly-synthesized fatty acids via NADPH, corresponding to a limited exchange with water hydrogen, but relatively low transfer via malonyl-CoA and acetyl-CoA intermediates indicating extensive hydrogen exchange at these loci of the DNL pathway.

Methods

Materials: [U-²H₇]- and [U-¹³C₆]glucose at 98-99% enrichment were obtained from Sigma-Aldrich. [3-²H]glucose at 98% enrichment was obtained from Omicron Biochemicals, South Bend, IN, USA.

Animal Studies: Animal studies were approved by the University of Coimbra Ethics Committee on Animal Studies (ORBEA) and the Portuguese National Authority for Animal Health (DGAV), approval code 0421/000/000/2013. Adult male C57BL/6 mice were obtained from Charles River Labs, Barcelona, Spain, and housed at the University of Coimbra Faculty of Medicine Bioterium, where they were maintained with a 12h light/12h dark cycle. Upon delivery to the Bioterium, mice were provided a two week interval for acclimation, with free access to water and standard chow. Following acclimation, the drinking water was supplemented with glucose and fructose (15.0 g of each sugar to 100g water). In the first set of studies, the glucose was enriched to 20% each with [U-²H₇]glucose and [U-¹³C₆]glucose. In a second set of studies, glucose was enriched to 16% each with [3-²H]glucose and [U-¹³C₆]glucose. In the third set of experiments, mice were administered an i.p. injection of 99.9% ²H₂O containing 9 mg NaCl per ml at a dose of 4 g/100 g body mass at the start of the dark period. For these animals, the drinking water was enriched to 5% with ²H₂O and the glucose was enriched to 50% with [U-¹³C₆]glucose but not with ²H. Animals were allowed to feed and drink *ad libitum* during the entire 12 hour dark period and were euthanized by cervical dislocation the following morning. Livers and adipose tissue depots were freeze-clamped and stored at -80°C until further processing for triglyceride extraction and purification.

Triglyceride extraction and purification: Liver triglyceride was extracted and purified as previously described (10). Briefly, livers were powdered under liquid nitrogen and then rapidly mixed with HPLC-grade methanol (4.6 mL/g) followed by methyl-tert-butyl ether (MTBE) (15.4 mL/g). The mixture was placed in a shaker for 1 hour at room temperature then centrifuged at

13,000 g for 10 min. The liquid fraction was collected and phase separation was induced by adding 4 mL of distilled water to the liquid fraction and letting it rest at room temperature for 10 min. The liquid was then centrifuged for 10 min. at 1,000 g. The upper organic phase containing the lipids was carefully separated and dried under nitrogen gas in a dark glass vial. Triglyceride from the dried lipid extracts were purified with a solid phase extraction (SPE) process. Discovery DSC-Si SPE cartridges (2g/12 ml) were washed with 8 mL of hexane/MTBE (96/4 v/v) followed by 24 mL of hexane. The dried lipids were re-suspended in 800 μ L of Hexane/MTBE (200/3; v/v) and added to the column after washing. The lipid vials were washed with a further 500 μ L solvent to quantitatively transfer the lipids to the column. Triglycerides were eluted with 32 mL of Hexane/MTBE (96/4; v/v), collected in 4 ml fractions. Fractions containing triglycerides were identified by thin-layer chromatography. A few microliters of the eluted fractions were spotted on the TLC plate alongside triglyceride standards and the plate was developed with petroleum ether/diethyl ether/acetic acid (7.0/1.0/0.1; v/v/v). After drying, lipid spots were visualized by iodine vapor. The triglyceride-containing fractions were pooled and dried under nitrogen gas and stored at -20°C until ready for NMR analysis.

NMR Analysis: Purified triglycerides were dissolved in ~ 0.5 ml CHCl_3 . To these, 25 μ l of a pyrazine standard enriched to 1% with pyrazine- d_4 and dissolved in CHCl_3 (0.07g pyrazine/g CHCl_3), and 50 μ l C_6F_6 were added. ^1H and ^2H NMR spectra were acquired with an 11.7 T Bruker Avance III HD system using a dedicated 5 mm ^2H -probe with ^{19}F lock and ^1H -decoupling coil as previously described. ^1H spectra at 500.1 MHz were acquired with a 90-degree pulse, 10 kHz spectral width, 3 seconds acquisition time and 5 seconds pulse delay. Sixteen free-induction decays (fid) were collected for each spectrum. ^2H NMR spectra at 76.7 MHz were obtained with a 90-degree pulse, a 1230 Hz sweep width, an acquisition time of 0.37 seconds and a pulse delay of 0.1 seconds. Between 10,000 and 20,000 fid were acquired for each spectrum. Correction factors were applied to all ^2H -triglyceride signals to adjust their intensities relative to the partially-saturated ^2H

pyrazine standard signal. These were obtained as mean values from a set of seven liver triglyceride samples obtained from mice administered with $^2\text{H}_2\text{O}$. For each sample, a spectrum was acquired with the described parameters and immediately followed by a spectrum acquired under the same parameters with the exception of the acquisition time and pulse delay, which were set to 1 second and 8 seconds, respectively. The correction factors for the ^2H signals in fatty acid position 2, position 3 and methyl hydrogens were 0.51, 0.52 and 0.88, respectively. For ^{13}C isotopomer analysis by ^{13}C NMR, dried triglyceride samples were dissolved in 0.2 ml 99.96% enriched CDCl_3 (Sigma-Aldrich) and placed in 3 mm NMR tubes. ^{13}C NMR spectra were acquired at 150.8 MHz with an Agilent V600 spectrometer equipped with a 3 mm broadband probe. Spectra were acquired with a 70° pulse, an acquisition time of 2.5 seconds, and a 0.5 second pulse delay. For each spectrum, 2,000-4,000 fid were collected.

Quantification of triglyceride positional ^2H - and ^{13}C -enrichments: Positional ^2H -enrichments of triglyceride fatty acids were quantified by analysis of ^1H and ^2H NMR triglyceride spectra as previously described (5, 10). From the methyl and carboxyl ^{13}C NMR resonances, positional ^{13}C -enrichments of fatty acids were estimated from the ratio of ^{13}C - ^{13}C -spin-coupled doublet signals (representing positional isotopomers derived from $[1,2-^{13}\text{C}_2]\text{acetyl-CoA}$) to the singlet signal, representing the 1.11% natural abundance ^{13}C (see Supplementary Figure 1). From the methyl singlet and doublet ^{13}C NMR signals, the ^{13}C -enrichment of fatty acids from $[1,2-^{13}\text{C}_2]\text{acetyl-CoA}$ in the methyl position was calculated as follows:

$$\text{Excess } ^{13}\text{C}\text{-enrichment of fatty acid methyls (\%)} = \mathbf{\text{Methyl D/Methyl S}} \times 1.11$$

Where **Methyl D** and **Methyl S** are the doublet and singlet components, respectively, of the ^{13}C -signal of the fatty acid terminal methyls and 1.11 represents the background ^{13}C -enrichment (%).

Assuming that fatty acid enrichment from [1,2- $^{13}\text{C}_2$]acetyl-CoA via elongation was limited to position 1 and 2 carbons, enrichment of carbon 3 were assumed to be equivalent to those of the terminal methyl carbon.

From analysis of the fatty acid singlet and doublet carboxyl ^{13}C -signals, excess enrichment of the position 1 of fatty acids from [1,2- $^{13}\text{C}_2$]acetyl-CoA was estimated as follows:

$$\text{Position 1 Excess } ^{13}\text{C}\text{-enrichment (\%)} = \frac{\Sigma \mathbf{D}}{\Sigma \mathbf{S}} \times 1.11$$

Where $\Sigma \mathbf{D}$ and $\Sigma \mathbf{S}$ are the summed doublet and singlet components, respectively, of the ^{13}C -carboxyl resonances and 1.11 represents the background ^{13}C -enrichment (%). Excess enrichment of the fatty acid position 2 carbon was assumed to be equal to that of position 1.

For determining the fractional rate of [U- $^2\text{H}_7$]glucose transfer into acetyl- and malonyl-CoA relative to that of [U- $^{13}\text{C}_6$]glucose, the $^2\text{H}/^{13}\text{C}$ enrichment ratios of the terminal methyl and carbon 2 positions were divided by 1.5 to account for the fact that there are three ^2H for every two ^{13}C in the initial glucose mixture. For estimating the fractional rate of [U- $^2\text{H}_7$]glucose transfer into NADPH relative to the lipogenic utilization of [U- $^{13}\text{C}_6$]glucose, we assumed that two ^2H were transferred per glucose molecule corresponding to one ^2H per acetyl-CoA derived from glucose.

Statistics: All results are presented as means \pm standard error and comparisons were made by an unpaired, two-tailed Student's t-test performed with Microsoft Excel.

Results:

Mice that were provided with the mix of [U- $^2\text{H}_7$]- and [U- $^{13}\text{C}_6$]glucose yielded liver triglycerides that were enriched in both ^{13}C and ^2H (Table 1). Both ^2H and ^{13}C NMR spectra featured composite signals of the inner fatty acid methylenes and well-resolved resonances representing both ends of

the fatty acid chain (Figure 2a, Supplementary Figure 1). Enrichment from [U-¹³C₆]glucose was relatively uniform between terminal and proximal carbons indicating that DNL was the main route for incorporation of glucose carbons into fatty acids with elongation playing a relatively insignificant role^a. In comparison, enrichment of fatty acid sites from [U-²H₇]glucose was highly heterogeneous, as seen by the very different intensities of positions 2 and 3 and the terminal methyl resonances (Figure 2a) and the excess ²H enrichments estimated from these signals (Table 1). Normalizing the fatty acid enrichment from [U-²H₇]glucose to that of [U-¹³C₆]glucose provides a measure of the fractional retention of the [U-²H₇]glucose ²H atoms in a given position (Table 2). These data reveal that for those fatty acids that were synthesized from exogenous glucose, far more ²H was transferred into the position 3 hydrogens compared to either position 2 or the terminal methyl hydrogens. This indicates a greater exchange of ²H and water hydrogens during the conversion of [U-²H₇]glucose to acetyl-CoA and malonyl-CoA compared to hydrogen transfer *via* PPP oxidation and NADPH. Only one of the fatty acid position 2 hydrogens is derived from malonyl-CoA, the other originates from body water. Therefore, based on the observed fatty acid position 2 ²H/¹³C enrichment ratio of 6%, we can infer that the ²H/¹³C enrichment ratio of the malonyl-CoA precursor was 12%. This is similar to the 14% estimated for the initial acetyl-CoA pool recruited by fatty acid synthase (FAS).

We performed an additional a set of studies where [U-¹³C₆]glucose was accompanied by [3-²H]glucose, where incorporation of ²H into fatty acids from this precursor occurs exclusively via NADPH. Taking into account the lower ²H/¹³C precursor enrichment (16% versus 20% for the [U-²H₇]glucose/[U-¹³C₆]glucose experiments) the fatty acid ¹³C-enrichment distributions were consistent with those of the [U-²H₇]glucose/[U-¹³C₆]glucose study. This indicates that for both studies, exogenous glucose had been utilized to the same extent for DNL. Figure 2b shows a representative ²H NMR spectrum of liver triglyceride from a mouse provided with the [3-²H]glucose/[U-¹³C₆]glucose mixture. In accordance with the predicted metabolic fate of the ²H-

^a If elongation had been a significant route for [U-¹³C₆]glucose incorporation, enrichment of the proximal fatty acid carbons would be significantly higher than that of the terminal carbons.

label, fatty acids were enriched in position 3 while enrichment of position 2 was not detectable and the terminal methyl had a vestigial ^2H signal. Given the substantial transfer of glucose hydrogens into the position 3 of fatty acid relative to position 2, it might be expected that for mice administered with $^2\text{H}_2\text{O}$, enrichment of fatty acid position 3 would also be less than that of position 2. However, as shown by Figure 2c, the intensities of position 2 and 3 signals were similar, and there was no significant difference between the ^2H -enrichments quantified for each site ($1.79 \pm 0.19\%$ and $1.81 \pm 0.19\%$ for positions 2 and 3, respectively).

Discussion

Since the pioneering studies of Beylot and co-workers (4, 6), $^2\text{H}_2\text{O}$ has been extensively used as a tracer for quantifying fractional DNL rates. From the beginning, it was understood that ^2H incorporation into fatty acids might be limited by a), incomplete exchange of body water and metabolite hydrogens and/or b), discrimination against the incorporation of ^2H into these precursors or intermediates of FAS due to kinetic isotope effects. In the present study, by quantifying fatty acid positional enrichments corresponding to the transfer of ^2H from $[\text{U-}^2\text{H}_7]\text{glucose}$ via acetyl-CoA, malonyl-CoA, and NADPH, the extent of glucose hydrogen exchange during its conversion to fatty acids via each intermediate was evaluated.

Exchange of glucose ^2H during the formation of acetyl-CoA and malonyl-CoA: Glycolysis of $[\text{U-}^2\text{H}_7]\text{glucose}$ yields one pyruvate with a single ^2H and a second pyruvate with two ^2H in the methyl position. Therefore, there are 1.5 equivalents of ^2H for each pyruvate. If this pyruvate is recruited for lipogenesis via acetyl-CoA, citrate and cytosolic acetyl-CoA, one of the methyl hydrogens undergoes obligatory exchange with water, resulting in one equivalent of ^2H per cytosolic acetyl-CoA. While pyruvate methyl hydrogens can undergo extensive exchange with water via alanine aminotransferase (11), there is evidence that not all intracellular pyruvate participates in this process. For example, in perfused rat hearts supplied with $[3\text{-}^2\text{H}_3, 1\text{-}^{13}\text{C}]\text{pyruvate}$, Funk et al.

observed a significantly higher retention of ^2H in lactate compared to alanine at 3 and 6 minutes of perfusion (12). Moreover, pyruvate molecules with ^2H in the methyl position may be metabolized at different rates to those without ^2H . In the same setting, $[\text{U-}^2\text{H}_7, \text{U-}^{13}\text{C}_6]\text{glucose}$ was less efficiently incorporated into the Krebs cycle compared to $[\text{U-}^{13}\text{C}_6]\text{glucose}$ (13), suggesting that the presence of ^2H in the methyl hydrogens of acetyl-CoA was attenuating its conversion to citrate *via* citrate synthase. Thus, while there is an efficient exchange mechanism for incorporating ^2H from water into the methyl sites of pyruvate, there may be intracellular pyruvate pools that do not experience this exchange. Moreover, pyruvate molecules that do become enriched with ^2H may be transformed into citrate and cytosolic acetyl-CoA at slower rates in comparison to their non-deuterated counterparts. In our study, we found that for the initial FAS-bound acetyl-CoA that was derived from exogenous $[\text{U-}^2\text{H}_7]\text{glucose}$, 86% of ^2H had been exchanged for ^1H . From analysis of cytosolic acetyl-CoA ^2H -enrichment from $^2\text{H}_2\text{O}$ via chemical biopsy, Duarte et al. concluded that exchange between the methyl hydrogens of this precursor and body water was $\sim 100\%$ (5). In our experimental setting, exogenous glucose contributes a minor fraction ($\sim 10\%$) of hepatic DNL (14). In the presence of $^2\text{H}_2\text{O}$ it is probable that endogenous DNL sources, including acetyl-CoA derived from fructose, lactate and microbial acetate, will be already enriched to a significant extent with ^2H prior to being recruited for DNL. For these reasons, we believe that the overall hydrogen exchange fraction of the lipogenic acetyl-CoA pool is closer to 100% than to 86%. Thus, in our experimental setting, animals provided with $^2\text{H}_2\text{O}$ would be expected to have near-equivalent ^2H -enrichments of acetyl-CoA methyl hydrogens and body water. For $[\text{U-}^2\text{H}_7]\text{glucose}$ that was metabolized to fatty acid via malonyl-CoA, exchange of ^2H with ^1H was similar to that observed for acetyl-CoA. Therefore, enrichment of malonyl-CoA from $^2\text{H}_2\text{O}$ would also be expected to approach that of body water.

^2H transfer from glucose to fatty acids via NADPH: ^2H that were metabolized from glucose to fatty acids via NADPH were more highly retained in comparison to those transferred via acetyl-

CoA and malonyl-CoA. During PPP oxidation, the first and third hydrogens of glucose are transferred to NADPH, hence [U- $^2\text{H}_7$]glucose contributes two ^2H while [3- ^2H]glucose only contributes one. In accordance, transfer of ^2H to fatty acid position 3 from [U- $^2\text{H}_7$]glucose was found to be approximately twice that from [3- ^2H]glucose (46% *versus* 22%, see Table 2). This indicates that under our study conditions, there was no additional loss of ^2H from glucose position 1 compared to position 3, for example by exchange of glucose-6-phosphate with fructose-6-phosphate and mannose-6-phosphate (15). Direct studies of intracellular NADPH enrichment from $^2\text{H}_2\text{O}$ report a greater degree of exchange between the reducing hydrogen and body water than might be expected based on our observations (16). One explanation for this is that the PPP is not the sole source of intracellular NADPH, as illustrated by Figure 3. In mitochondria, NADPH can be generated from NADH by nicotinamide nucleotide transhydrogenase. In mitochondria as well as cytosol, NADPH can also be generated via NADP^+ -malic enzyme and NADP^+ -isocitrate dehydrogenase. In all of these cases, the likelihood that the hydrogen that was transferred to NADP^+ had previously exchanged with body water is high. For NADPH formed via the NADP^+ -malic enzyme, the reducing hydrogen originates from hydrogen 2 of malate, which in turn originated from water during the hydration of fumarate. If the malate is metabolized via the Krebs cycle to citrate and isocitrate, this hydrogen is transferred to NADPH via NADP^+ -isocitrate dehydrogenase. The bulk of mitochondrial NADH hydrogens are also derived from Krebs cycle intermediates such as malate, whose hydrogens are highly exchanged with those of water. In addition, NADPH and water hydrogens may also be exchanged via NADP^+ -linked redox enzymes (16, 17). Another consideration, and an important caveat of our assessment of hydrogen exchange at the level of NADPH, is that fatty acid ^2H enrichment from [U- $^2\text{H}_7$]glucose via this pathway was quantified relative to [U- $^{13}\text{C}_6$]glucose conversion to fatty acid via malonyl-CoA. If the rate of glucose oxidation by the PPP was different to that of its conversion to fatty acid via malonyl-CoA, then the fractional rate of $^2\text{H}/^1\text{H}$ exchange at the level of NADPH would also differ from the $^2\text{H}/^{13}\text{C}$

ratio of fatty acid position 3^b. However, this does not alter the conclusion that the relative amounts of ²H transferred from glucose to fatty acid via NADPH were significantly higher than those transferred via acetyl-CoA and malonyl-CoA intermediates.

Our observation of extensive ²H transfer from glucose to fatty acid synthesis via NADPH suggests that this process is tightly coupled to the extent that NADPH generated by PPP does not fully mix with other intracellular NADPH pools. This apparent compartmentation of PPP and lipogenic NADPH metabolism has also been reported in other laboratories using different isotopic approaches and models. In mice with fatty liver, hepatic PPP fluxes measured by a ¹³C-isotopomer approach were found to be highly correlated with lipogenesis but were not associated with antioxidant activity (18). This suggests that in the postprandial liver, NADPH derived from PPP is prioritized for DNL rather than being utilized for antioxidant defense such as the reduction of oxidized glutathione. In the H1299 tumour cell line supplied with various ²H-enriched substrates, Lewis et al. also demonstrated a substantial transfer of ²H label from [3-²H]glucose to fatty acids, while fatty acid ²H-enrichment via NADPH from [2,3,3-²H₃]serine was much more limited (19).

Fatty acid enrichment from ²H₂O: We observed extensive exchange of exogenous glucose hydrogens with water during its conversion to fatty acids via both acetyl- and malonyl-CoA. In contrast, glucose hydrogens that were transferred to fatty acids *via* NADPH experienced more limited exchange. Based on these observations, it would be anticipated that enrichment of the fatty acid position 2 hydrogens from ²H₂O - derived from water and malonyl-CoA - would be equivalent to those of body water, while those of position 3 - derived via NADPH - would be significantly less enriched. Instead, we observed that positions 2 and 3 were enriched to the same level. As mentioned previously, exogenous glucose is a minor contributor of acetyl-CoA to DNL in our experimental setting (although it may have a more substantial contribution to the NADPH

^b For example, if the rate of glucose oxidation via PPP was twice the rate of glucose conversion to fatty acid via malonyl-CoA, then NADPH ²H enrichment would be one-half of the fatty acid position 3 ²H/¹³C ratio (i.e 23% compared to 46%).

equivalents for DNL). Moreover, following $^2\text{H}_2\text{O}$ administration under both fed and fasted conditions, hepatic glucose-6-phosphate becomes highly enriched with ^2H in all positions due to extensive cycling between glucose-6-phosphate and gluconeogenic precursors (20, 21). Under these conditions, NADPH derived from PPP oxidation of glucose-6-phosphate will also become highly enriched with ^2H and this will be transferred to the respective fatty acid positions.

Implications for estimating the number of deuterium atoms incorporated per fatty acid (N): Under our study conditions, the number of deuterium atoms incorporated per fatty acid molecule (N) appears to approach the theoretical value (i.e. 31 for palmitate). Therefore in this instance, no correction needs to be applied to the observed fatty acid ^2H enrichment from $^2\text{H}_2\text{O}$. This differs from previous studies in rats, where N was estimated to be 21 and 22 out of 31 (68% and 71% of the theoretical value) by mass isotopomer distribution analysis (MIDA) for plasma and liver triglyceride palmitate, respectively (6, 7). To our knowledge, N has not been determined in the mouse by MIDA, but given its smaller size and higher basal metabolic rate, it might be expected to be higher compared to the rat. The mice in our study also ingested significant amounts of fructose, a sugar that is rapidly metabolized via triose phosphate intermediates to glucose-6-phosphate, lactate and acetyl-CoA thereby further promoting ^2H -enrichment of these metabolites from $^2\text{H}_2\text{O}$. It is possible that for mice fed a standard chow diet featuring maltose as the main carbohydrate component – whose digestion yields unlabeled glucose - there could be less complete ^2H incorporation from $^2\text{H}_2\text{O}$ into fatty acids, particularly via NADPH. In cultured cells, N for palmitate was estimated to be 17 (8). This is 55% of the theoretical value and is also substantially lower than that determined for *in vivo* rat studies. Our data for mice indicate that if glucose was the sole source of DNL *in vivo*, the value of N would be 24 based on ^2H transfer from exogenous [$^2\text{H}_7$]glucose to fatty acids via acetyl-CoA, malonyl-CoA and NADPH^c. Since there is more opportunity for the loss of glucose ^2H by Cori cycling and other inter-organ transfer of glucose

^c For palmitate, this is calculated as $31 - [(3 \times 0.14) + (14 \times 0.46) + (7 \times 0.06)]$.

metabolites *in vivo* compared to *in vitro*, we anticipate that there would be a greater degree of transfer of ^2H from glucose to fatty acids *in vitro*, corresponding to a lower N value.

In conclusion, N may vary considerably according to the type of organism as well as the substrates that were utilized for DNL. Our study indicates that transfer of hydrogen from unlabelled glucose to fatty acids via NADPH is an important factor in the non-stoichiometric incorporation of ^2H into fatty acids during DNL. For the measurement of DNL with $^2\text{H}_2\text{O}$, the ratio of ^2H -enrichment in fatty acid positions 2 and 3 as measured by ^2H NMR provides a convenient internal check for assessing the extent to which this might have occurred.

Acknowledgements: The authors acknowledge financial support from the Portuguese Foundation for Science and Technology (research grants PTDC/SAU~MET/11138/2009, EXCL/DTP/0069/2012 and FCT-FEDER-02/SAICT/2017/028147). Structural funding for the Center for Neurosciences and Cell Biology and the UC-NMR facility is supported in part by FEDER – European Regional Development Fund through the COMPETE Programme and the Portuguese Foundation for Science and Technology through grants POCI-01-0145-FEDER-007440; REEQ/481/QUI/2006, RECI/QEQ-QFI/0168/2012, CENTRO-07-CT62-FEDER-002012, and Rede Nacional de Ressonancia Magnética Nuclear. GDW is supported by the European Union's Horizon 2020 Research and Innovation programme under the Marie Skłodowska-Curie Grant Agreement No. 722619 (Project FOIE GRAS).

Footnotes:

- a) If elongation had been a significant route for $[\text{U-}^{13}\text{C}_6]$ glucose incorporation, enrichment of the proximal fatty acid carbons would be significantly higher than that of the terminal carbons.

- b) For example, if the rate of glucose oxidation via PPP was twice the rate of glucose conversion to fatty acid via malonyl-CoA, then NADPH ^2H enrichment would be one-half of the fatty acid position 3 $^2\text{H}/^{13}\text{C}$ ratio (i.e 23% compared to 46%).
- c) For palmitate, this is calculated as $31 - [(3 \times 0.14) + (14 \times 0.46) + (7 \times 0.06)]$.

References

1. Forcheron, F., A. Cachefo, S. Thevenon, C. Pinteur, and M. Beylot. 2002. Mechanisms of the triglyceride- and cholesterol-lowering effect of fenofibrate in hyperlipidemic type 2 diabetic patients. *Diabetes* **51**: 3486-3491.
2. Diraison, F., P. Moulin, and M. Beylot. 2003. Contribution of hepatic *de novo* lipogenesis and reesterification of plasma non esterified fatty acids to plasma triglyceride synthesis during non-alcoholic fatty liver disease. *Diabetes & Metabolism* **29**: 478-485.
3. Saponaro, C., M. Gaggini, and A. Gastaldelli. 2015. Nonalcoholic fatty liver disease and type 2 diabetes: common pathophysiologic mechanisms. *Current Diabetes Reports* **15**.
4. Diraison, F., C. Pachiaudi, and M. Beylot. 1997. Measuring lipogenesis and cholesterol synthesis in humans with deuterated water: Use of simple gas chromatographic mass spectrometric techniques. *Journal of Mass Spectrometry* **32**: 81-86.
5. Duarte, J. A. G., F. Carvalho, M. Pearson, J. D. Horton, J. D. Browning, J. G. Jones, and S. C. Burgess. 2014. A high-fat diet suppresses *de novo* lipogenesis and desaturation but not elongation and triglyceride synthesis in mice. *Journal of Lipid Research* **55**: 2541-2553.
6. Diraison, F., C. Pachiaudi, and M. Beylot. 1996. In vivo measurement of plasma cholesterol and fatty acid synthesis with deuterated water: determination of the average number of deuterium atoms incorporated. *Metabolism: Clinical & Experimental* **45**: 817-821.
7. Lee, W. N., S. Bassilian, H. O. Ajje, D. A. Schoeller, J. Edmond, E. A. Bergner, and L. O. Byerley. 1994. *In vivo* measurement of fatty acids and cholesterol synthesis using D₂O and mass isotopomer analysis. *American Journal of Physiology* **266**: E699-E708.
8. Lee, W. N., S. Bassilian, Z. Guo, D. Schoeller, J. Edmond, E. A. Bergner, and L. O. Byerley. 1994. Measurement of fractional lipid synthesis using deuterated water (²H₂O) and mass isotopomer analysis. *American Journal of Physiology* **266**: E372-E383.

9. Delgado, T. C., D. Pinheiro, M. Caldeira, M. Castro, C. Geraldes, P. Lopez-Larrubia, S. Cerdan, and J. G. Jones. 2009. Sources of hepatic triglyceride accumulation during high-fat feeding in the healthy rat. *NMR in Biomedicine* **22**: 310-317.
10. Viegas, I., I. Jarak, J. Rito, R. A. Carvalho, I. Meton, M. A. Pardal, I. V. Baanante, and J. G. Jones. 2016. Effects of dietary carbohydrate on hepatic *de novo* lipogenesis in European seabass (*Dicentrarchus labrax L.*). *Journal of Lipid Research* **57**: 1264-1272.
11. Walter, U., H. Luthe, F. Gerhart, and H. D. Soling. 1975. Hydrogen-exchange at beta-carbon of amino-acids during transamination. *European Journal of Biochemistry* **59**: 395-403.
12. Funk, A. M., X. Wen, T. Hever, N. R. Maptue, C. Khemtong, A. D. Sherry, and C. R. Malloy. 2019. Effects of deuteration on transamination and oxidation of hyperpolarized ¹³C-Pyruvate in the isolated heart. *Journal of Magnetic Resonance* **301**: 102-108.
13. Funk, A. M., B. L. Anderson, X. D. Wen, T. Hever, C. Khemtong, Z. Kovacs, A. D. Sherry, and C. R. Malloy. 2017. The rate of lactate production from glucose in hearts is not altered by per-deuteration of glucose. *Journal of Magnetic Resonance* **284**: 86-93.
14. Silva, J.C.P., C. Marques, F.O. Martins, I. Viegas, L. Tavares, M.P. Macedo, and J.G. Jones. 2019. Determining contributions of exogenous glucose and fructose to *de novo* fatty acid and glycerol synthesis in liver and adipose tissue. *Metabolic Engineering* **56**: 69-76.
15. Chandramouli, V., K. Ekberg, W. C. Schumann, J. Wahren, and B. R. Landau. 1999. Origins of the hydrogen bound to carbon 1 of glucose in fasting: significance in gluconeogenesis quantitation. *American Journal of Physiology* **277**: E717-723.
16. Zhang, Z., L. Chen, L. Liu, X. Su, and J. D. Rabinowitz. 2017. Chemical basis for deuterium labeling of fat and NADPH. *Journal of the American Chemical Society* **139**: 14368-14371.

17. Fan, J., J. Ye, J. J. Kamphorst, T. Shlomi, C. B. Thompson, and J. D. Rabinowitz. 2014. Quantitative flux analysis reveals folate-dependent NADPH production. *Nature* **510**: 298-302.
18. Jin, E. S., M. H. Lee, R. E. Murphy, and C. R. Malloy. 2018. Pentose phosphate pathway activity parallels lipogenesis but not antioxidant processes in rat liver. *American Journal of Physiology* **314**: E543-E551.
19. Lewis, C. A., S. J. Parker, B. P. Fiske, D. McCloskey, D. Y. Gui, C. R. Green, N. I. Vokes, A. M. Feist, M. G. Vander Heiden, and C. M. Metallo. 2014. Tracing compartmentalized NADPH metabolism in the cytosol and mitochondria of mammalian cells. *Molecular Cell* **55**: 253-263.
20. Delgado, T. C., F. O. Martins, F. Carvalho, A. Goncalves, D. K. Scott, R. O'Doherty, M. P. Macedo, and J. G. Jones. 2013. ^2H enrichment distribution of hepatic glycogen from $^2\text{H}_2\text{O}$ reveals the contribution of dietary fructose to glycogen synthesis. *American Journal of Physiology* **304**: E384-391.
21. Bederman, I. R., S. Foy, V. Chandramouli, J. C. Alexander, and S. F. Previs. 2009. Triglyceride synthesis in epididymal adipose tissue: contribution of glucose and non-glucose carbon sources. *Journal of Biological Chemistry* **284**: 6101-6108.

Table 1: Fatty acid ^{13}C and ^2H enrichments from one group of mice provided with glucose enriched to 20% with $[\text{U-}^{13}\text{C}_6]$ - and $[\text{U-}^2\text{H}_7]$ glucose and a second group provided with glucose enriched to 16% with $[\text{U-}^{13}\text{C}_6]$ - and $[\text{3-}^2\text{H}]$ glucose.

<i>Experiment</i>	<i>Isotope</i>	Fatty acid Positional enrichment		
		<i>Methyl</i>	<i>Position 2</i>	<i>Position 3</i>
20% $[\text{U-}^{13}\text{C}_6]$ glucose + 20% $[\text{U-}^2\text{H}_7]$ glucose (n=11)	^{13}C	0.99 ± 0.06	$1.04 \pm 0.07^\#$	$0.99 \pm 0.06^*$
	^2H	0.23 ± 0.02	0.09 ± 0.01	0.49 ± 0.05
16% $[\text{U-}^{13}\text{C}_6]$ glucose + 16% $[\text{3-}^2\text{H}]$ glucose (n=5)	^{13}C	0.77 ± 0.02	0.83 ± 0.03	0.77 ± 0.02
	^2H	0.01 ± 0.01	n.d.	0.17 ± 0.02

$^\#$ ^{13}C -Excess enrichment of fatty acid position 1 carboxyl carbons was assumed to be equivalent to that of position 2.

* ^{13}C -Excess enrichment of fatty acid position 3 was assumed to be equivalent to that of the methyl carbon.

n.d. = not detected (signal to noise ratio < 3:1).

Table 2: $^{13}\text{C}/^2\text{H}$ Enrichment ratios for fatty acid positions 2, 3 and methyls estimated from the group of eleven mice provided with $[\text{U-}^2\text{H}_7]$ - and $[\text{U-}^{13}\text{C}_6]$ glucose and that of fatty position 3 from the group of five mice provided with $[\text{3-}^2\text{H}]$ - and $[\text{U-}^{13}\text{C}_6]$ glucose.

Fatty acid positional $^2\text{H}/^{13}\text{C}$ enrichment ratios			
	<i>Position 2</i>	<i>Position 3</i>	<i>Methyl</i>
$[\text{U-}^2\text{H}_7]/[\text{U-}^{13}\text{C}_6]$ glucose	$0.06 \pm 0.01^*$	$0.46 \pm 0.04^{**}$	0.14 ± 0.01
$[\text{3-}^2\text{H}]/[\text{U-}^{13}\text{C}_6]$ glucose	not determined	0.22 ± 0.02	not determined

$^*p < 0.005$ compared to methyl.

$^{**}p < 10^{-5}$ compared to methyl.

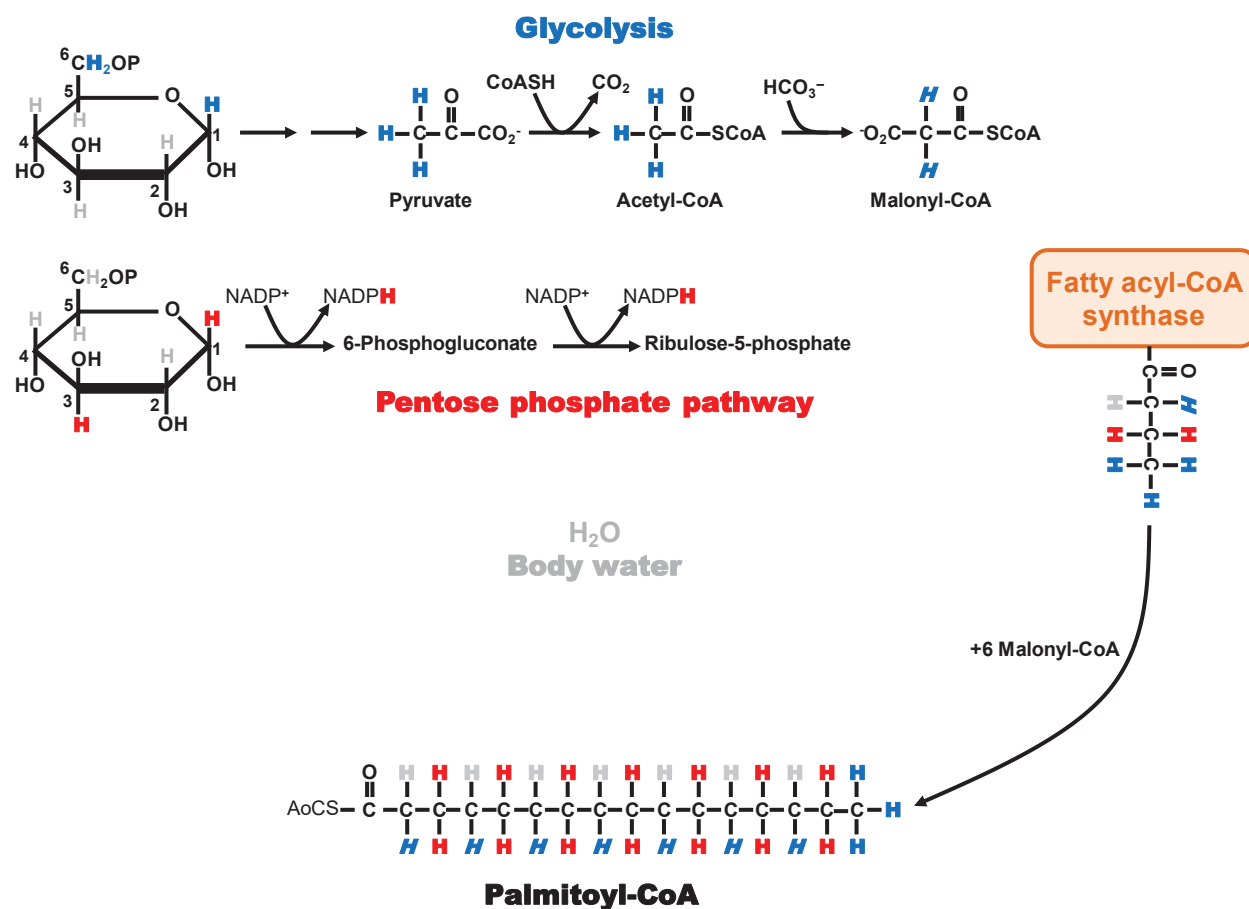


Figure 1: Sources of hydrogens for the synthesis of palmitoyl CoA from glucose and body water via fatty acyl-CoA synthase, with the butyryl-ACP intermediate also shown. When glucose is metabolized via glycolysis, hydrogens 1 and 6 shown in blue, are transferred to pyruvate then to acetyl-CoA and malonyl-CoA (represented by blue italic). During the first cycle of fatty acid synthesis, acetyl-CoA and malonyl-CoA hydrogens are incorporated into the terminal methyl group and one of the position 2 hydrogens of butyryl-ACP, respectively. In the palmitoyl-CoA product, this corresponds to the terminal methyl hydrogens and one of the methylene hydrogens attached to each even-numbered carbon. When glucose is metabolized via the pentose phosphate pathway, hydrogens 1 and 3, shown in red, are transferred to NADPH. During the first cycle of fatty acid synthesis, these are incorporated into both position 3 hydrogens of butyryl-ACP and subsequently into both methylene hydrogens attached to each odd-numbered carbon of palmitoyl-CoA. The remaining hydrogen in position 2 of butyryl-ACP is derived from body water, shown in grey, and is incorporated into one of the methylene hydrogens attached to each even-numbered carbon of palmitoyl-CoA. The colour scheme indicates possible labeling sites only and is not meant to represent the stoichiometry of hydrogen transfer.

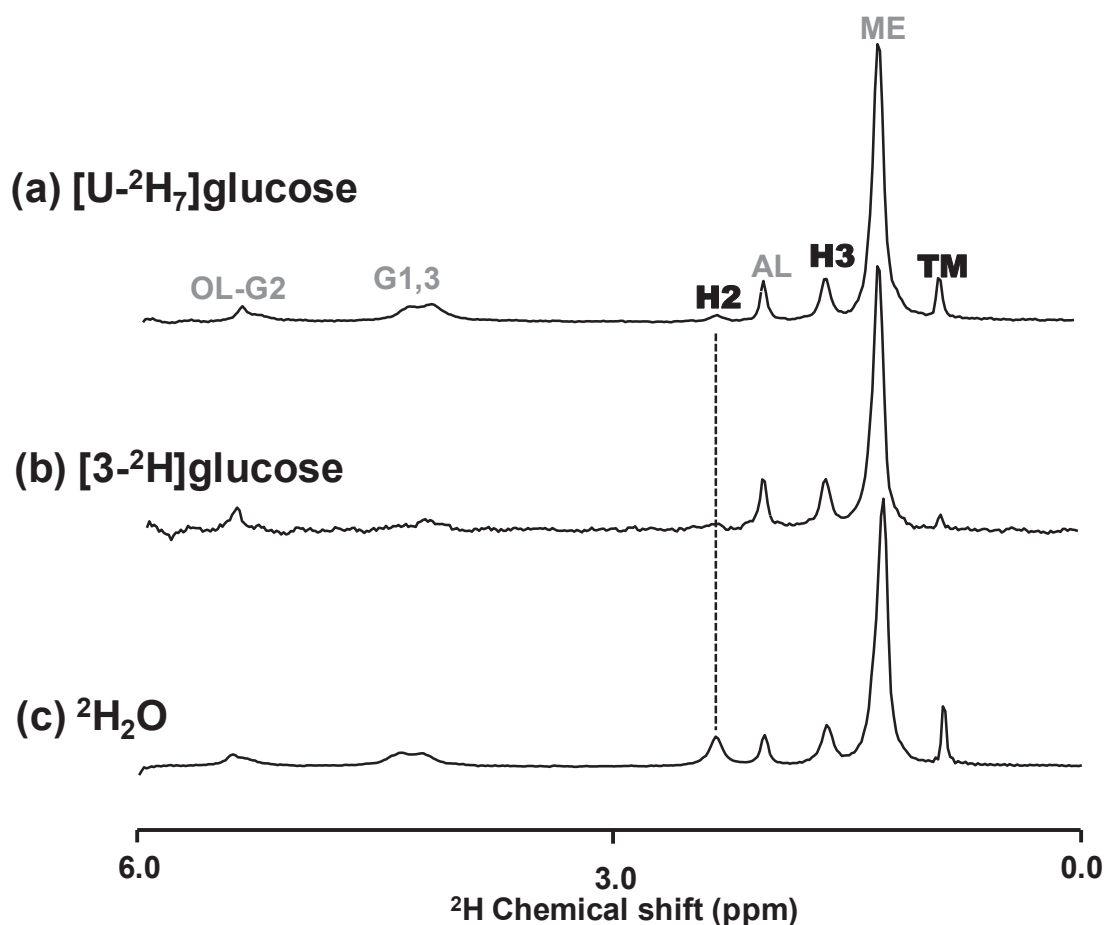


Figure 2: a) A representative ^2H NMR spectrum of purified liver triglyceride acquired from a mouse provided with glucose enriched with equimolar amounts of $[\text{U-}^2\text{H}_7]\text{glucose}$ and $[\text{U-}^{13}\text{C}_6]\text{glucose}$, b), a ^2H NMR spectrum of triglyceride acquired from a mouse provided with glucose enriched with equimolar amounts of $[\text{3-}^2\text{H}]\text{glucose}$ and $[\text{U-}^{13}\text{C}_6]\text{glucose}$, and c), a ^2H NMR spectrum of triglyceride acquired from a mouse provided with $^2\text{H}_2\text{O}$ and $[\text{U-}^{13}\text{C}_6]\text{glucose}$. For the spectra, the signals corresponding to ^2H in the fatty acid terminal methyl (**TM**), as well as in fatty acid position 2 (**H2**) and position 3 (**H3**) are indicated in bold. Also indicated are signals from ^2H in fatty acid olefinic sites and glycerol position 2 (**OL-G2**), ^2H from glycerol *sn*1,3 positions (**G1,3**), ^2H bound to the allylic carbon of monounsaturated fatty acids (**AL**) and ^2H bound to the inner methylene carbons (**ME**).

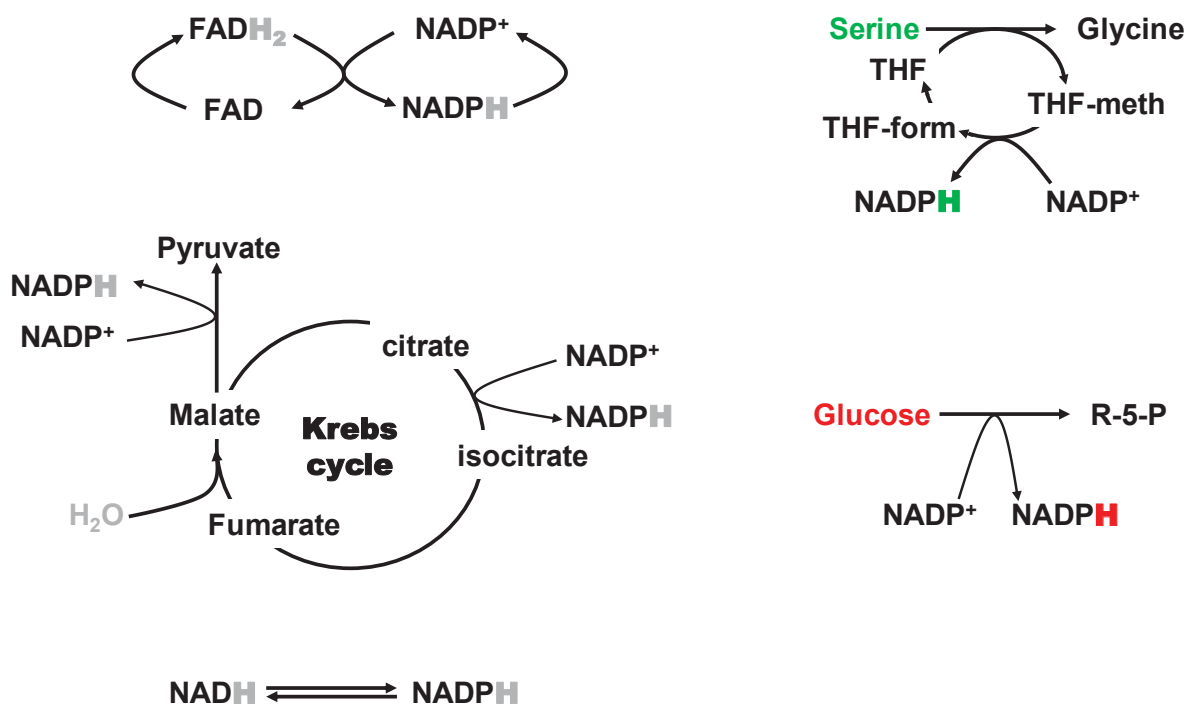


Figure 3: Schematic of intracellular NADPH hydrogen sources. On the left-hand side are the pathways that are involved in the transfer of water hydrogen to NADPH, depicted in grey. These include cycling between NADPH and other redox co-factors such as FAD whose hydrogens are exchanged with those of water; generation of NADPH from malate and isocitrate via $NADP^+$ -malic enzyme and $NADP^+$ -isocitrate dehydrogenase, respectively; and exchange of NADH and NADPH via transhydrogenase. On the right hand side are the two principal pathways that transfer hydrogens to NADPH from nutrient substrates, namely glucose and serine.